

MEASUREMENTS OF STRAIN-RATE DISTRIBUTIONS ON MATERIAL AFTER SHPB IMPACT

M. Kawai¹⁾, M. Futakawa²⁾, T. Naoe²⁾,
H. Yamada³⁾, and C.N. Xu³⁾

¹⁾ **High Energy Accelerator Research Organization**

Tsukuba, Ibaraki-ken 305-0801, Japan
e-mail: masayoshi.kawai@kek.jp

²⁾ **J-PARC Center, Japan Atomic Energy Agency**

Tokai-mura, Ibaraki-ken 319-1195, Japan

³⁾ **National Institute of Advanced Industrial Science and Technology (AIST)
AIST Kyushu**

Tosu, Saga-ken 841-0052, Japan
e-mail: cn-xu@aist.go.jp

We have proposed a sophisticated novel method of the SHPB experiment to measure the local strain-rate distributions on a surface of the specimen by using mechanoluminescent materials combined with a high-speed camera and an image intensifier. The feasibility study was made for the aluminum specimens pasted by a typical mechanoluminescent material -Eu doped SrAl₂O₄ film, in order to obtain the fundamental data for the method. Our results showed that SrAl₂O₄: Eu emitted lights as a response to the stress. Increase of the light intensity was swift enough to follow the strain change due to SHPB impact. The luminescence intensity was experimentally verified and expressed as a product of strain and strain rate. Accordingly, it can be said that this method gives a good tool for measuring time variation of local strain distributions.

1. INTRODUCTION

The Split Hopkinson Pressure Bar (SHPB) technique is widely used to measure a stress-strain relation of materials with a well-controlled impact loading of a specimen. Recently some new SHPB test methods were developed together with analysis by numerical simulations [1, 2] because deformation of the specimen extends the range of elasticity due to very high strain-rate, or specimen of soft materials such as nylon. For new materials of limited quantities, multi-section striker method was developed by combining numerical simulation to save an amount of material to be tested [3]. Various SHPB experiments were

reported for composite materials characterized by non-uniform media [4–6]. Experiments for particle reinforced metal matrix composite (such as SiCp/2024Al composite) showed that composite’s strength was weakened by adiabatic heat and cumulative damage under high strain rate compression [4]. Characterization of carbon-fiber reinforced 3D waves was made by tensile loading and shear loading in the SHPB experiments, providing the data for failure and damage behavior [5]. Unidirectional carbon/epoxy laminated composites were investigated to obtain a compressive stress-strain curves up to failure [6].

In the conventional SHPB experiment, strain and strain-rate of a specimen can be calculated from pulse data measured by strain gages mounted on the input and output bars with an assumption of homogeneous deformation of the specimen. Thus, the calculated strain and strain-rate are those of the specimen as a whole. In the case followed by failure and damage, anisotropic 3D and especially local strain, seems to play an important role in crack initiation. Accordingly, in order to analyze the mechanism to the failure and damage due to impact, it will be necessary to measure such local strains. A novel method of photography measuring 3D deformation of the specimen in the SHPB experiments was developed by M.R. ARTHINGTON [7], using a high-speed camera and mirrors. Trial experiment was made on Ti-6Al-4V specimen assuming that material strength was dependent on the rolling direction [8]. The cylindrical specimen was deformed to elliptic with SHPB loading, and major and minor radii of an ellipse were measured by detecting the edge of the image taken by the camera as a function of the axial position and time. The data were compared with the results of a finite element analysis. Spall test of glass-fibre reinforced polymers was also made using a Hopkinson bar configuration together with a high-speed camera [9].

Even in these novel techniques, the local strain can be hardly measured, because it is very difficult for experimentalists to distinguish, with a high accuracy, local deformations from an image caught by the high-speed camera. Additionally, the method to measure the strain-rate has not been reported as yet. The research group of Chao-Nan Xu, one of the authors, has developed a smart material with a property to emit lights the intensity of which is proportional to stresses given to the material, that is called a mechanoluminescence material [10–12]. If we paste a proper mechanoluminescent material on the specimen of the SHPB experiment, it will emit lights corresponding to the strain and strain-rate of the specimen. Accordingly, we will be able to directly obtain the data for strain and strain-rate distributions on the surface of the specimen from the light image, which will be taken by a high-speed camera. In the present work, we have investigated the applicability of the method, by selecting a typical mechanoluminescence material, Eu doped SrAl_2O_4 as a sensor of the SPH experiments, to give the time-dependent strain distributions.

2. EXPERIMENTS

A plane-strain wave incident experiment was carried out using a modified split Hopkinson bar impact technique for aluminum specimens with surfaces pasted by a $\text{SrAl}_2\text{O}_4:\text{Eu}$ film, as shown in Table 1. The cylindrical specimen 16 mm high and 8 mm in diameter was placed between the stainless-steel input and output bars of 16 mm in diameter and 1.5 meter in length, as shown in Fig. 1.

Table 1. List of the method of pasting $\text{SrAl}_2\text{O}_4:\text{Eu}$ on the aluminum specimen.

Identification	Method
AL-2-F-2	To paste inconel sheet with sputtered $\text{SrAl}_2\text{O}_4:\text{Eu}$
AL-3-G	To paste aluminum film with sprayed $\text{SrAl}_2\text{O}_4:\text{Eu}$
AL-4-3	To spray $\text{SrAl}_2\text{O}_4:\text{Eu}$ directly on aluminum specimen
AL-1-3	To paste aluminum film with screen-printed $\text{SrAl}_2\text{O}_4:\text{Eu}$

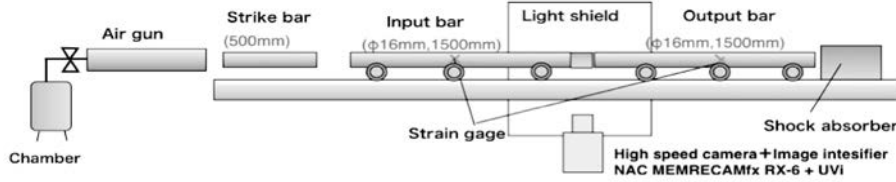


FIG. 1. Schematic of a modified SHPB apparatus.

In a conventional SHPB, an assumption is made that a uniaxial homogeneous stress distribution is produced along the axial direction of the specimen and the forces imposed on both ends of the bars are equal. Then the average nominal strain $\varepsilon(t)$, strain rate $\dot{\varepsilon}(t)$ and stress $\sigma(t)$ in the specimen are obtained from the reflected strain $\varepsilon_r(t)$ and transmitted strain $\varepsilon_t(t)$, measured in the Hopkinson bars as follows:

$$(2.1) \quad \varepsilon(t) = \frac{-2c_0}{l_s} \int_0^t \varepsilon_r(t') dt',$$

$$(2.2) \quad \dot{\varepsilon}(t) = \frac{-2c_0}{l_s} \varepsilon_r(t),$$

$$(2.3) \quad \sigma(t) = \frac{EA}{A_s} \varepsilon_t(t),$$

where A is the cross-sectional area, c_0 the longitudinal elastic wave velocity of the Hopkinson bars, E the Young modulus of the bars, and A_s and l_s are the cross-sectional area and the gage length of the specimen.

Picture of luminescence from $\text{SrAl}_2\text{O}_4\text{:Eu}$ after the SHPB impact was taken by a high-speed camera NAC MEMRECAMfx RX-6 with a condition of 20 000 frames per second during 40 μs exposure, by multiplying light intensity with image intensifier NAC UVi.

3. EXPERIMENTAL RESULTS AND DISCUSSIONS

Initially, impact tests were performed for the same AL-4-3 specimen, characterized by direct spaying, under a condition of loading velocity of the striking bar from 2.66 m/s, 4.10 m/s and 5.32 m/s, by controlling the air pressure in a chamber. Light emission was observed at the loading velocities of 4.10 m/s and 5.32 m/s, while not observed at 2.66 m/s. Accordingly, other specimens were tested at the loading velocity of about 4 m/s and light emission was observed for AL-3-G and AL-1-3. The specimen with inconel film did not shine because of smaller strain due to high modulus of the inconel. Figure 2 shows the pictures at a time when luminescence intensity became the highest. It is found that the luminescence has broad two-dimensional distributions the peak of which appears at the output-bar side from the center of the specimen, except for the case of AL-3-G-002. The case of AL-4-3-003, which had a weak remaining luminescence due to the previous impact test for AL-4-3-002, shows a slightly weaker luminescence in the figure. Dark region in the lower part of a left-hand side (output-bar side) was due to grease fixing the specimen to the experimental apparatus.

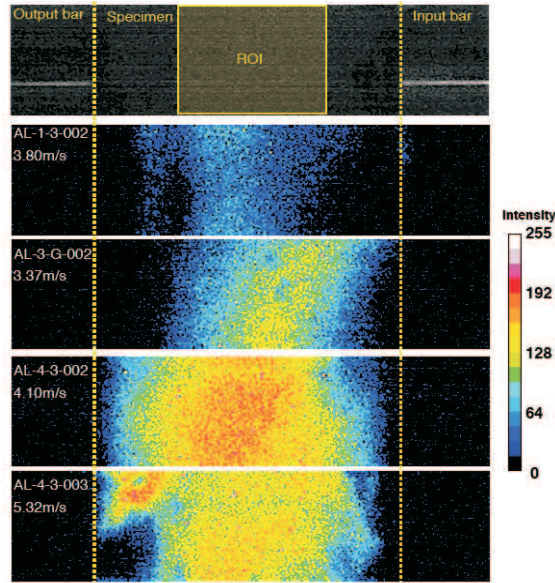


FIG. 2. Picture of peak luminescence.

Figure 3 compares time variation of mean intensity of luminescence among 4 cases. All cases show a quite swift rise-up and decay within 0.5 ms. After that, slow decaying follows over 10 ms. From the figure, it can be said that the method of direct spraying a mechanoluminescence material on the specimen is better than other, because mean intensity of the AL-4-3 specimens are higher than the other specimens.

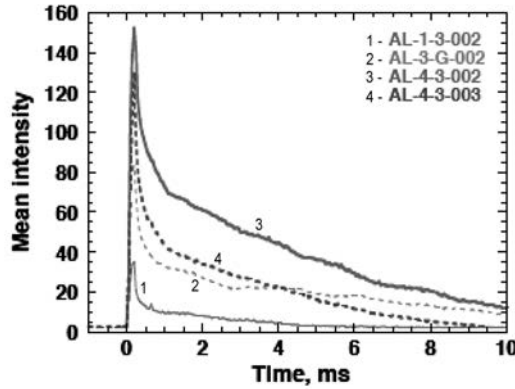


FIG. 3. Time variation of mean intensity of luminescence.

Figure 4 shows the AL-4-3-002 luminescence distribution change with time after the SHPB impact along the central horizontal lines, where the light intensity became the highest. Horizontal distribution is moving, according to movement of the specimen location, towards the output bar. The growing area also changes by getting narrow. These luminescence distribution change will be useful to understand the deformation behaviour of the specimen.

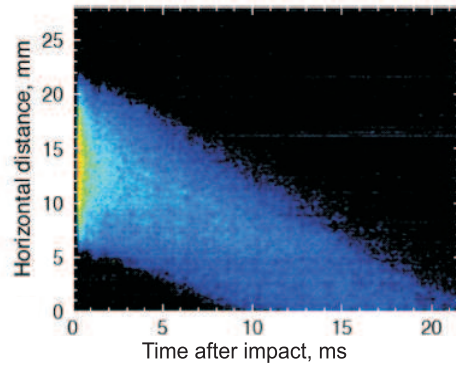


FIG. 4. Luminescence distribution along the central horizontal line.

Figure 5 shows the strain data of ε_i , ε_r and ε_t measured by the strain gages at the input and output bars after the SHPB impact. According to Eq. (2.1),

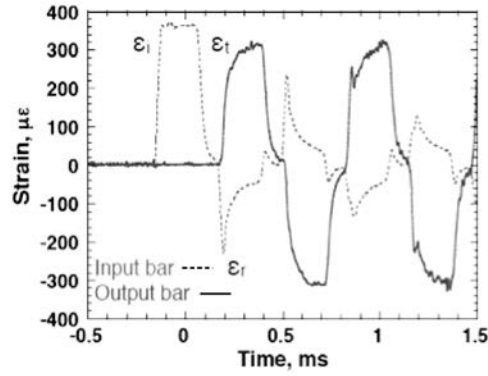


FIG. 5. Measured strain data.

the strain values of the specimen were calculated as a function of time after the impact. Calculated results compared with luminescence intensity are shown in Fig. 6. In this figure, the relation between the strain and intensity is not obvious in individual cases, even such as made with similar impact loading. The difference must result from different method of pasting $\text{SrAl}_2\text{O}_4:\text{Eu}$ on the specimen. Accordingly, it seems to difficult to be derive any quantitative rule between them.

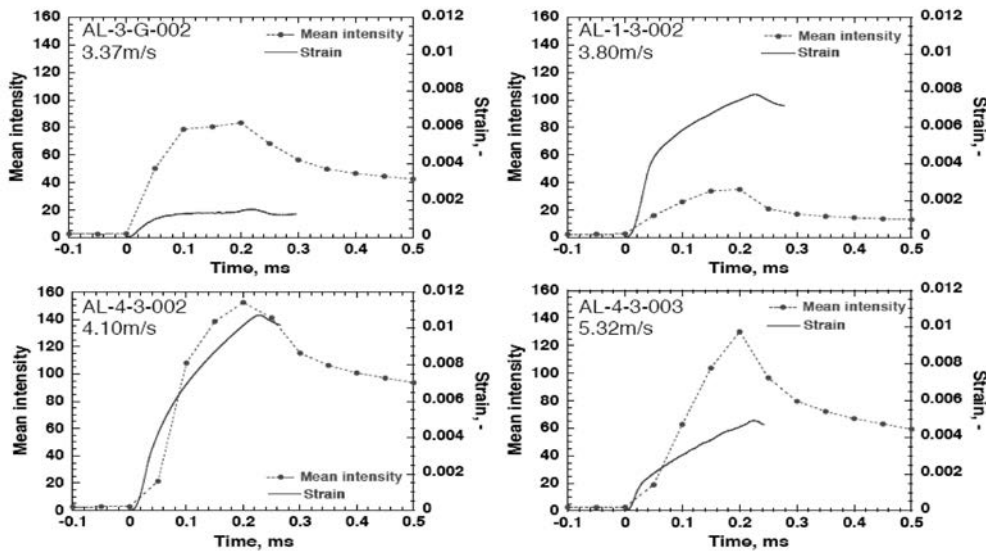


FIG. 6. Comparison of the strain and luminescence as a function of time.

On the other hand, for cases using the same specimen AL-4-3 it is noted that the latter case AL-4-3-003, even with a larger impact, showed a smaller strain and weaker luminescence than the former case AL-4-3-002. The latter case may be influenced by plastic deformation due to an over-loading beyond elastic

deformation region after the test of the AL-4-3-002. Thus, luminescence may suggest more clearly the type of deformation of the specimen than the strain.

CHAO-NAN XU [11] has derived the following relation between the luminescence intensity and strains:

$$(3.1) \quad S_{ML} = C_0 \varepsilon \frac{d\varepsilon}{dt},$$

where, C_0 is the normalization factor.

We applied the above equation, together with Eqs. (2.1) and (2.2), to the case of AL-4-3-002. The calculated luminescence intensity is compared with the experimental one in Fig. 7. Quite good similarity is observed up to the peak at 0.2 ms after the SHPB impact in the figure. This result indicates that the Eq. (3.1) is applicable even to the present swift deformation phenomena.

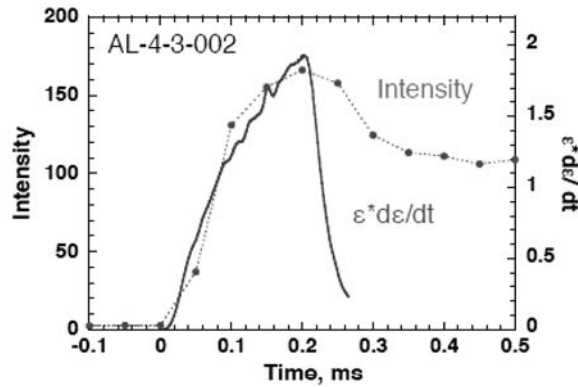


FIG. 7. Comparison of the calculated luminescent intensity with the experimental data.

At a time after the peak, experimental luminescence shows a slow decay. Such decay components are the appearance of an inherent property of the mechanoluminescence materials, and it will be possible to remove the contamination of the remaining luminescence in the pixel-wise from the picture by assuming a decay mode, which can be evaluated at a time properly elapsed from the peak time.

Thus, it can be said that the mechanoluminescence gives us information on the strain phenomena exactly composed of a product of strain and strain rate, and has a possibility to measure a time-dependent local strain distributions. On the other hand, K. ANDERSON [14] has reported the grating technique to measure three-dimensional strain using stereo cameras. The technique is used to determine the three-dimensional deformation and the tangential strain of sheet metal. A grating is fixed on the surface and taken by stereo-cameras in different deformation states. By suitable line-following software, the grating coordinates

in the images are determined with subpixel accuracy. Using photogrammetric methods, the three-dimensional coordinates are calculated from the image coordinates. The strain is usually determined by means of a deformation gradient, which is calculated from every deformed triangle. Thus, we will be able to evaluate the strain-rate by subtracting the effect of the strain data measured with high-speed stereo-cameras from the measured luminescence distributions.

4. CONCLUSION

We have proposed a sophisticated novel method of the SHPB experiments to measure the local strain-rate distributions by using a mechanoluminescence materials, combined with a high-speed camera and image intensifier. The feasibility study was made for the aluminum specimens with a typical mechanoluminescence material, Eu doped SrAl_2O_4 film, in order to obtain the fundamental data for the method. Results showed that $\text{SrAl}_2\text{O}_4:\text{Eu}$ emitted lights with response to the strain on the sample surface. The rise of the light intensity was swift enough to follow the strain due to the SHPB impact. It was also verified that the luminescence intensity was expressed as a product of strain and strain-rate, even in the swift deformation such as the SHPB experiments.

Accordingly, the present method can be said to give a good tool to measure local strain-rate distributions by applying a technique to measure the strain displacements with high-speed stereo cameras. Further experiments will be needed to confirm the reliability and to improve the method by selecting a better mechanoluminescence materials, as well as developing a data-acquisition and -processing system, obtaining a local strain distributions in the SHPB experiment. If we manage to develop a more sensitive sensor, swifter phenomena with in microsecond will be also observable by using a suitable high-speed camera and image-intensifier. Wider application will be also possible in the field of mechanical dynamics experiments [13]. The results will clarify the reliability of the fundamental Eqs. (2.1) to (3.1) in the SHPB experiments and the phenomena leading cracks.

ACKNOWLEDGMENT

This research was supported by a Grant-in-Aid in Scientific Research Category (S) by the Japan Society for Promotion of Science, No. 19106017.

REFERENCES

1. L. WANG, H. LAI and J. ZHU, *Studies on high strain-rate behavior of materials by using a new method combining HPB technique with Lagrangian analysis*, Proceedings of the 9th

International Conference on the Mechanical and Physical Behavior of Materials under Dynamic Loading (DYMAT 2009), Vol. 1, pp. 43–49, 2009, ISBN: 978-2-7598-0472-6.

2. T. UMEDA and K. MIMURA, *Accurate measurement of stress-strain relation under high strain rate condition by using non-coaxial Hopkinson bar method*, *ibid.*, **1**, 127–134, 2009.
3. A. BOUAMOUL, M. BOLDUC and R. ARSENAUT, *Development of multi-section striker for split Hopkinson bar experiments and numerical simulation*, *ibid.*, **1**, 149–154, 2009.
4. Y. ZHU, B. PANG, B. GAI, L. WANG and W. ZHANG, *Dynamic compressive behavior of 45 vol.% SiCp/2024Al composite at various strain rate*, *ibid.*, **1**, 155–161, 2009.
5. R. GELACH, C. R. SIVIOUR, N. PETRINIC, and J. WIEGAND, *Experimental characterization of the strain rate dependent failure and damage behavior of 3D composite*, *ibid.*, **1**, 219–225, 2009.
6. T. YOKOYAMA and K. NAKAI, *Impact compressive failure of a unidirectional carbon/epoxy laminated composite in three principal material directions*, *ibid.*, **1**, 639–646, 2009.
7. M. R. ARTHINGTON, C. R. SIVIOUR, N. PETRINIC, and B. C. F. ELLIOTT, *Cross-section reconstruction during uniaxial loading*, *Measurement Science and Technology*, **20**, 075701, 2009.
8. E. WIELEWSKI, C. R. SIVIOUR, N. PETRINIC, M. R. ARTHINGTON and S. CARTER, *Taylor impact experiments on Ti-6Al-4V specimens using 3D geometry reconstruction and instrumented target rods*, *Proceedings of the 9th International Conference on the Mechanical and Physical Behavior of Materials under Dynamic Loading (DYMAT 2009)*, **1**, 257–263, 2009.
9. R. GOVENDER, L. LOUCA, A. PULLEN and G. NURICK, *High strain rate delamination of glass fibre reinforced polymers using a Hopkinson bar configured for spalling*, *ibid.*, **1**, 449–455, 2009.
10. C. N. XU, T. WATANABE and M. AKIYAMA, *Direct view of stress distribution in solid by mechanoluminescence*, *App. Phys. Letters*, **74**, 2414–2416, 1999.
11. C. N. XU, *Coating*, [in:] *Encyclopedia of SMART Materials*, Mel Schwarits [Ed.], John Wiley & Sons, Inc., **1**, 190–201, 2002.
12. C. N. XU, H. YAMADA, X. WANG and X. G. ZHENG, *Strong elastico-luminescence from monoclinic structure SrAl₂O₄*, *App. Phys. Letters*, **84**, 3040–3042, 2004.
13. C. N. XU, *Sensing technology with elastico-luminescence* [in Japanese], *Ceramics Japan*, 154–160, 2009.
14. K. ANDERSON, *Strain tensor for large three-dimensional surface deformation of sheet metal from an object grating*, *Experimental Mechanics*, **39**, 30–35, 1999.

Received December 20, 2010; revised version April 14, 2011.
